THz QCLs for heterodyne receivers and wavelength modulation spectroscopy

Alan W.M. Lee*[a], Tsung-Yu Kao [a], Ian A. Zimmerman [a], William T.S. Cole[b], Richard Thurston[b], Richard J. Saykally[b], Ningren Han[c], Qing Hu[c]
[a] LongWave Photonics LLC, 958 San Leandro Ave, Mountain View, CA, USA 94043; [b]University. of California, Berkeley, CA, USA 94720; Massachusetts Institute of Technology, Cambridge, MA 02139

ABSTRACT

Milliwatt average power terahertz quantum cascade lasers (THz-QCLs, 2 THz to 5 THz) have been developed for spectroscopy and as local oscillators for heterodyne receivers. Novel DFB THz-QCLs have been fabricated and show single-mode operation. The narrow line widths of <10 MHz and stark shift tuning of of 6 GHz, allows for wavelength modulation spectroscopy of low pressure gasses in the unexplored THz frequency band. The same devices also act as local-oscillators for heterodyne receivers for remote-sensing and astronomy. Lastly we report on improved tunable DFB devices for use in spectroscopy.

Keywords: terahertz quantum cascade laser, spectroscopy, heterodyne

1. INTRODUCTION

Missions such as Aura (EOS CH-1)/MLS (Microwave Limb Sounder), SOFIA/GREAT and STO have demonstrated the need for local oscillator (LO) sources between 30 and 300 μm (1 and 10 THz) [1-4]. Sensitive heterodyne receivers for these missions typically use local oscillators (LOs) based on electronic sources for detectors below 2 THz. However resistive and capacitive and transit time effects in these sources limit their available power to microwatt levels above 2 THz [5]. This is insufficient to pump Schottky diode mixers (1 mW) and is at the minimum required power level for superconducting hot electron bolometer (HEB) mixers (>10 μW including coupling losses). These requirements are further strained for arrays of detectors which scale scaling super linearly with the number. Above 2 THz, platforms such as EOS/AURA have used discrete lines provided by gas laser based local oscillators [6]. While the power levels of these devices can be >10 mW at certain frequency transitions, these sources are large, consume large amounts of power, cannot be continuously frequency tuned and have long-term stability issues that require complicated stabilization. As an alternative, a source with the following features is highly desirable [3, 6-7]: continuous-wave (CW) power output of >1 mW with single-mode operation, frequency-locked to within the detector IF bandwidth of the target gas (approximately <6 GHz), longterm frequency stability of ~100 kHz, frequency agility, allowing for the detection of multiple gas species, and a low size, weight and power consumption (SWaP).

As an alternative to electronic or gas laser based LOs, Terahertz Quantum-Cascade Laser (QCL) sources show promise as a compact, easy to use source of light from 2 to 5 THz, fulfilling many of these requirements. These semiconductor lasers have no moving parts and have demonstrated power levels of >1 W [8], have shown tunable devices [9-10], and have been demonstrated for spectroscopy [11]. Additionally, these devices have shown improved operating temperatures up to 200 K -- making them compatible with compact closed cycle cryoccoolers [12]. These devices have been fabricated in distributed feedback (DFB) lasers for use as local oscillators in heterodyne receivers [13-14]. In this work, we present a compact, closed cycle cooling system operable with an array of DFB THz QCLs, frequency locking of the DFBs to a reference gas cell, and applications to basic science. Lastly we report on an all-electronic tunable QCL for frequency agility.

2. THZ QCL SYSTEMS

2.1 3rd Order DFB QCLs

The THz QCL gain media used in this work is based on the resonant phonon design [15]. To obtain single-mode operation, and control the emission frequency of a QCL, a distributed feedback (DFB) grating fabricated into a metal-

*awmlee@longwavephotonics.com; phone 617 399 6405; fax 617 399 6406; www.longwavephotonics.com

Micro- and Nanotechnology Sensors, Systems, and Applications VIII, edited by Thomas George, Achyut K. Dutta, M. Saif Islam, Proc. of SPIE Vol. 9836, 98362O · © 2016 SPIE
CCC code: 0277-786X/16/$18 · doi: 10.1117/12.2224158

metal waveguide can be used [16]. First-order gratings, where the grating periodicity, Λ, is half a guided wavelength ($\Lambda \approx \lambda/2$) have been demonstrated in single-mode operation. However, the subwavelength dimensions of the optical waveguide result in highly divergent beam patterns exceeding 180°. A unique solution to control the beam divergence has been demonstrated using third-order gratings [17]. Here the grating corrugations are spaced at $\Lambda \approx 3 \cdot \lambda/2$, where λ is equal to λ_o/n, the freespace wavelength divided by the optical index of the GaAs/GaAlAs multiple quantum wells (MQW) gain medium, typically n~3.5-3.6. This makes $\Lambda \approx \lambda_o/2$, effectively making the laser an end-fire linear antenna array. To enhance the outcoupling of these devices, antenna structures have been fabricated at the $\Lambda \approx \lambda_o/2$ spacings, as shown in Figure 1 part (a) [18]. Characteristics for a typical device fabricated at 3.8 THz are shown in part (b), which shows power level of 1.15 mW with a power consumption of 1.7 W of DC power. Emission frequency is single mode (part c) with a symmetric beam pattern (part d). The operating temperature for these devices is typically 45 to 55 K, and are compatible with compact crycooler systems as shown in (part e), which are <12 kg and operate with less than 250 W DC power, in a 48 × 22 × 17 cm^3 form factor for convenient laboratory use.

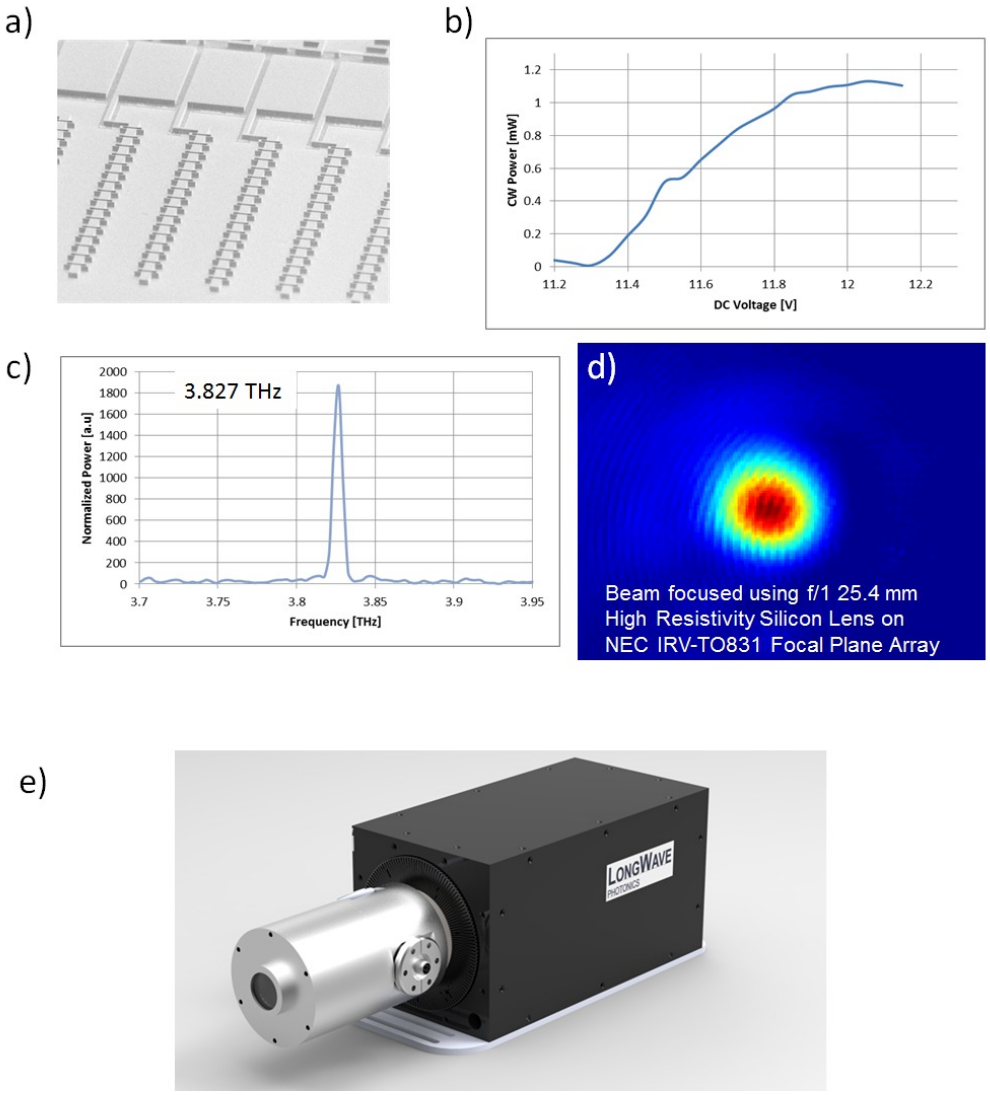

Figure 1. Part (a) shows SEM of DFB QCL. Typically 15 to 20 devices are fabricated monolithically, with small frequency variations across the array ensuring that a frequency precision of <6 GHz, the typical IF bandwidth of a heterodyne receiver. Part (b) shows CW measurement of power versus device voltage with the single-mode emission spectrum shown in part (c). Part (d) shows the focused beam pattern on a focal-plane array detector (NEC IRV-TO831). DFB QCL is typically close cycle cooling in a Stirling cooler shown in part (e).

2.2 Frequency Tuning and Spectroscopy

To stabilize the emission frequency of the DFB QCL, a reference cell frequency locking scheme is implemented as shown in Figure 2. As the beam of the DFB QCL passes through the gas cell, any frequency changes result in differing amounts of absorption by the reference gas, effectively converting frequency noise to amplitude noise. The minimum linewidth obtainable from this system can be described by the following equation:

$$\Delta f = \frac{df}{dV} \cdot \frac{dV}{dS} \cdot \sigma_{detector}$$

Here Δf is the laser linewidth, $\frac{df}{dv}$ is the frequency tuning constant of the laser with respect to voltage. The term $\frac{dS}{dV}$ is the change in signal, S, from the detector with respect to laser bias voltage after the beam has passed through the gas cell (i.e. a frequency discriminator), and σ_detector is the noise from the detector. In order to determine the laser linewidth, all three of these terms must be determined. This was done experimentally using methanol (CH3OH) at a pressure of 2 Torr where a balance between linewidth and absorption depth was found. Methanol was chosen because of the density of absorption lines—approximately 5 lines per GHz of tuning.

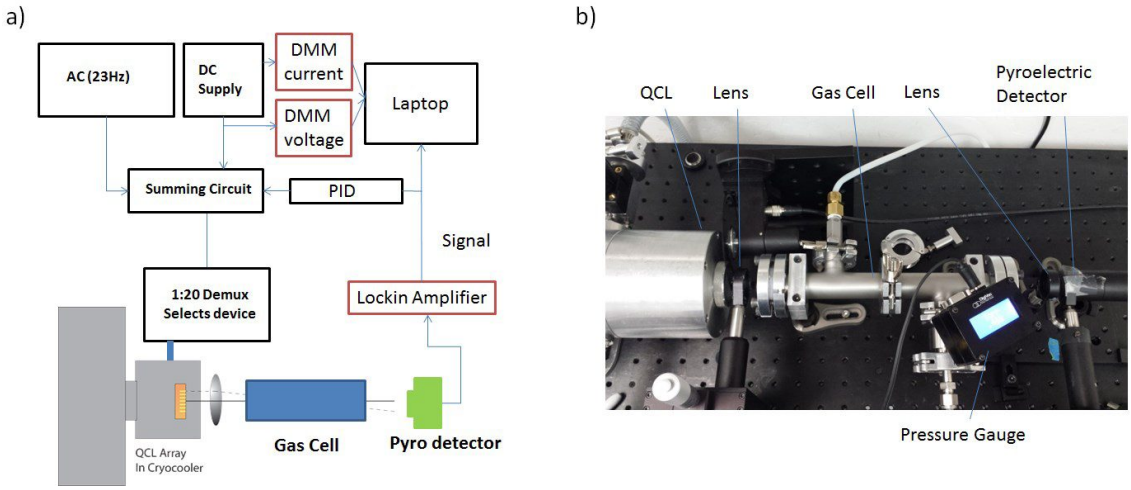

Figure 2: Part (a) Schematic of the frequency locking experiment. The DFB QCL in the cryocooler is frequency locked to a reference gas in the gas cell. The DFB QCL is FM modulated with a small AC signal superimposed on a DC bias. When the laser is tuned to the peak of a gas absorption line, the FM modulation results in an error signal from the pyroelectric detector. The error signal is fed into a PID controller to lock to the gas absorption peak. Part (b) shows frequency locking experimental setup.

Emission frequency of the QCL is dependent on the bias voltage due to the quantum confined stark effect (QCSE) and index of refraction temperature dependence. To determine the laser tuning constant, direct absorption spectroscopy is performed on methanol resulting in measurement of absorption versus voltage. This spectrum is then matched to a calculated spectrum to convert the voltage to frequency. Direct absorption spectroscopy is performed by routing a DC bias (no AC bias or PID control used in this experiment) via the demultiplexing circuit to a DFB QCL. The output beam of the QCL is optically chopped, passes through the reference cell, and is detected with a room temperature pyroelectric detector. The signal is then measured with a lock in amplifier referenced to the chopping frequency. Spectra are taken by sweeping the DC voltage of the QCL: once with the reference gas in the cell, and again with an empty cell for background normalization. Measurements with a single DFB QCL are shown in Figure 3 part (a) (here voltage has been converted to frequency as described below).

The measured spectra are compared with the JPL Millimeter and Submillimeter Spectral Line Catalog calculated spectra (part a). A fit of the calculated absorption peaks with the observed absorption peaks using a linear function of voltage is shown in part (b) [19]. This linear fit gives a laser bias tuning constant of 6.38 GHz/V. This tuning constant was

qualitatively verified by measuring the emission frequency of the DFB QCL versus bias in an FTIR setup as shown in part (c). A fit of the peak emission versus voltage (part d) results in a tuning constant of 7.5 GHz/V. Here the FTIR resolution is 6 GHz (FWHM), and the total tuning range is approximately 2 GHz, therefore the tuning constant obtained by FTIR is extremely coarse, and is only used to give approximate agreement with the number obtained by gas cell measurement.

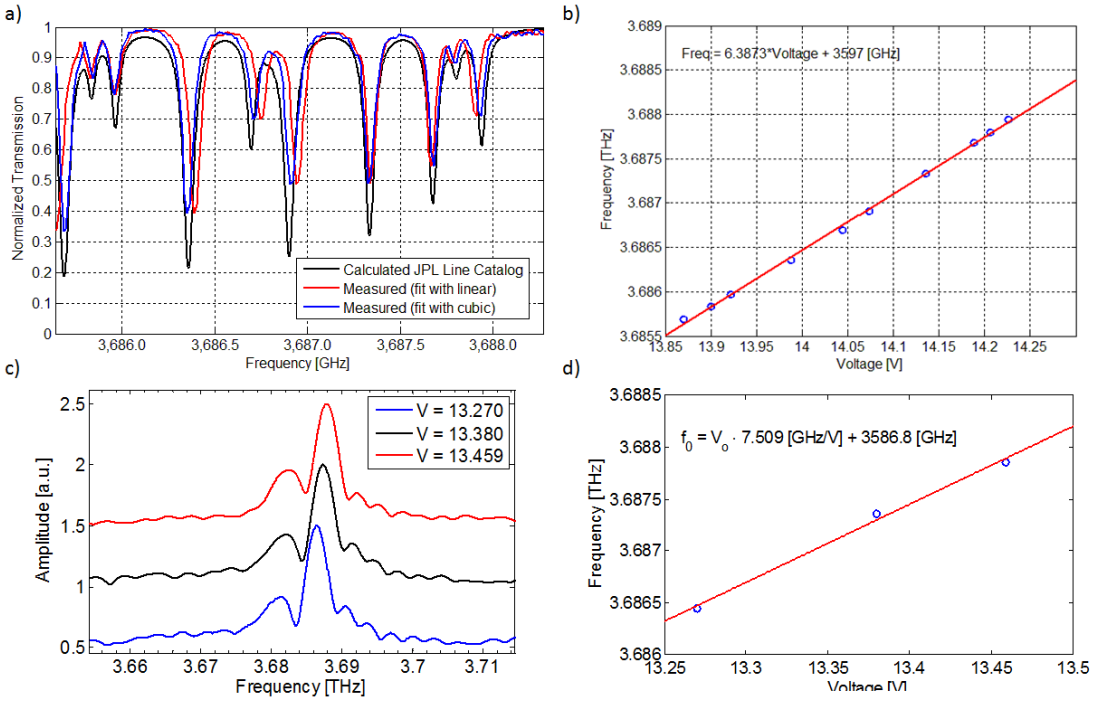

Figure 3: Part (a) shows measured direct absorption spectra of CH3OH at 2 Torr fit to JPL Line Catalog. A linear fitting function (part b) derived by matching observed and calculated absorption peaks is used to convert the laser bias voltage to output frequency of the laser. FTIR measurements of emission frequency versus voltage (part c) result in similar linear fit (part d), slightly offset due to different biasing conditions.

In addition to the optically chopped absorption measurements, 1-f wavelength modulation spectroscopy (WMS) on methanol is done. The resulting signal acts as a frequency discriminator for PID feedback in the frequency locking experiment described below. Here a small AC signal (10 mV, peak to peak) is added via a summing circuit to a DC supply voltage and routed via a demultiplexing circuit to bias to a DFB QCL. The AC bias provides a small amount of frequency modulation (FM), which results in the measurement of the first derivative (slope) of the gas absorption lines as shown in Figure 4. The first derivative of the absorption line works well as an error signal for frequency stabilization since it is relatively linear, and provides stable negative feedback when the frequency is either too low or too high. Using the laser tuning constant of 6.38 GHz/V, the 1-f frequency discriminator slope is linearly fit to 0.76 mV/MHz i.e. the lock in amplifier signal will change by 0.76 mV for a frequency deviation of 1 MHz.

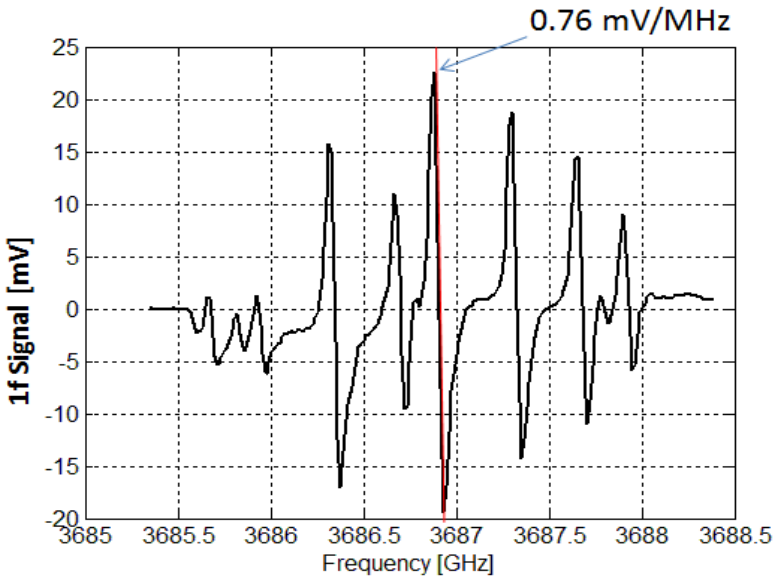

Figure 4: 1-f wavelength modulation spectroscopy signal of 2-Torr CH3OH gas cell. Line marked in red is used as the frequency discriminator for frequency locking.

To frequency lock, the 1-f signal is used as an error signal is fed into a PID controller and summed with the DC signal to provide feedback to the DFB QCL. Results from this frequency locking are shown from the pyroelectric detector signal shown in Figure 5. Part (a) shows the detector signal as a function of time for three operating conditions: free running, frequency locked, and free running with beam blocked (for detector noise characterization). The free running signal was observed to have a standard deviation of 1.78 mV and baseline movement ~10 mV over 200 seconds, which are equivalent to free running frequency standard deviation of 2.32 MHz and baseline drift of 13 MHz, respectively. If the experiment were run for longer periods of time, this frequency would continue to drift which is seen in a slowly varying baseline signal. When the PID loop is engaged, the frequency is locked with a standard deviation of 1.58 MHz. Long term frequency drift is countered by the output of the PID which is plotted in part (b). To ensure that the observed signal is due to frequency noise, and not detector noise, the detector was characterized by blocking the beam and disabling the PID control. The resulting detector signal has a standard deviation of 0.2 mV or 0.265 MHz i.e. the minimum measurable frequency deviation is approximately 0.265 MHz.

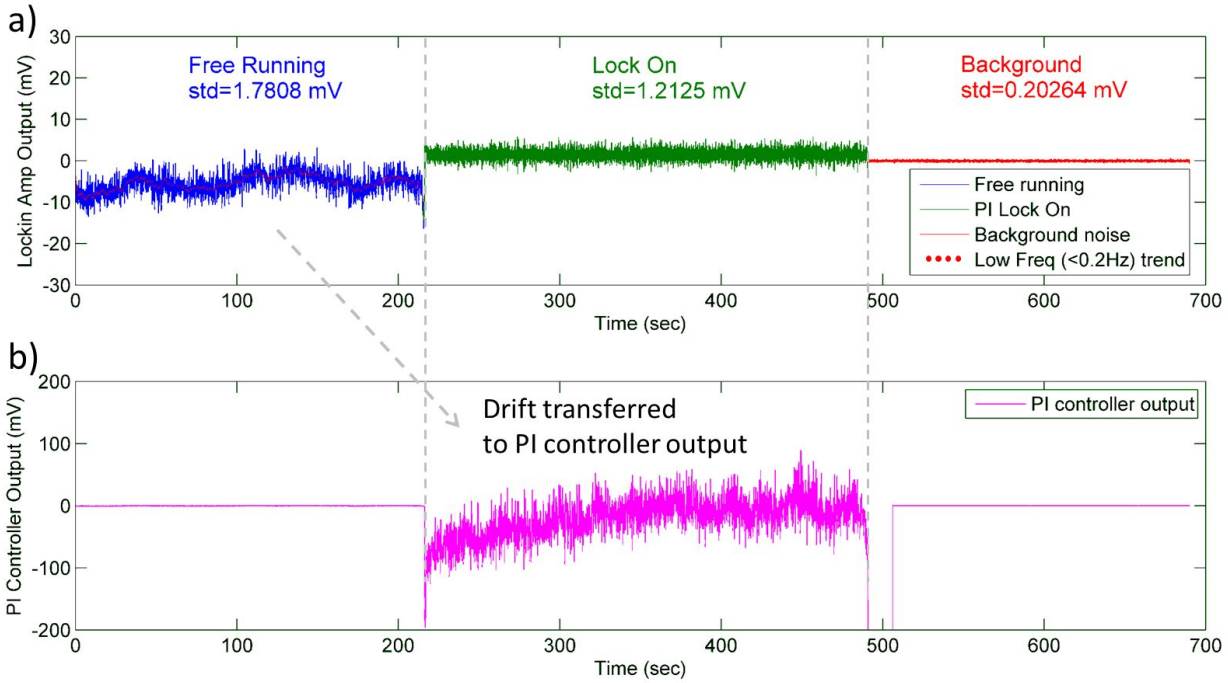

Figure 5: Part (a) shows pyroelectric detector output after passing through frequency discriminator (i.e. frequency noise is now converted to amplitude noise) versus time for free running QCL (t = 0 to 220 s), frequency locked (t = 220 to 490 s) and with the QCL beam blocked (t > 490 s). Part (b) shows the PID output signal, which effectively cancels long term drift when the system is frequency locked.

The cancellation of long term frequency drift can be seen from spectral density plots calculated by the Fourier transforms of the measured signals in the free running, PI locked, and the background detector only states (Figure 6). The free running state has a strong 1/f component which is effectively cancelled by the PID loop. From part (b) it can be seen that the DC component is effectively driven to noise floor of the detector.

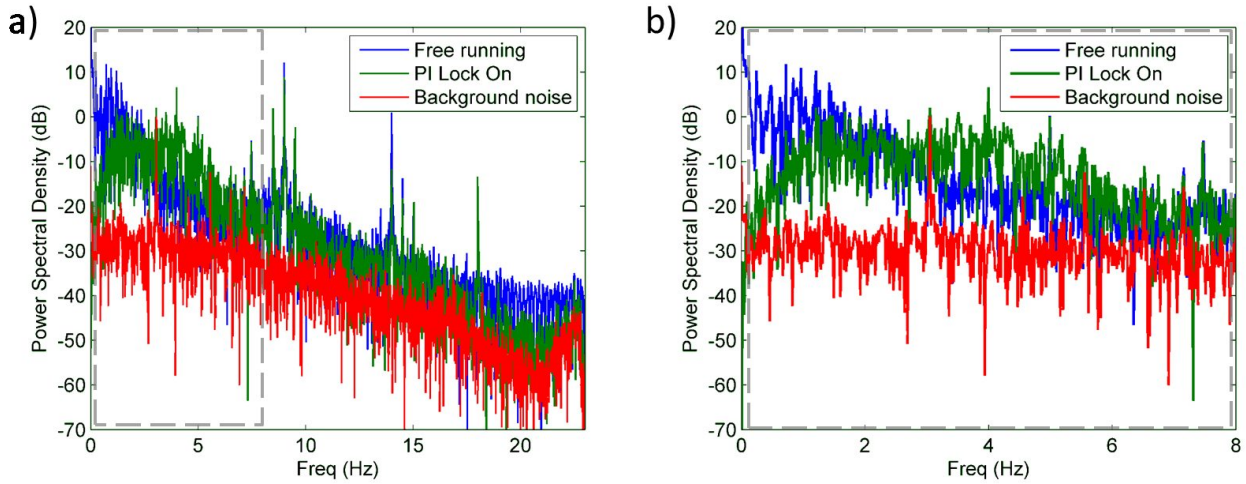

Figure 6: Part (a) shows spectral density plots of the detector signals. Free running shows highest noise at DC due to 1/f noise. When the system is frequency locked, the DC component is driven to the noise floor determined by the background noise. Part (b) shows an expanded version of part a.

The resulting frequency lock has three results: knowledge of the QCL emission frequency, reduction of linewidth to a value comparable to the specification for the LO on Aura/MLS (which required +/- 1 MHz) and elimination of baseline frequency drift. To improve on this gas cell frequency lock, the system could either: reduce the laser tuning constant, improve the frequency discriminator, or reduce the detector noise. Reduction of the laser tuning constant is difficult but possible. It is related to the position of the DFB frequency relative to the peak frequency of the gain medium. It has been observed that DFB lasers based on the same gain medium have a factor of 4 less frequency tuning (1.49 GHz/V) when lasing at 3.43 THz [20]. Little effort was made to optimize the frequency discriminator, and additional reductions in linewidth could likely be gained by changing the gas pressure and cavity length. Lastly the detector NEP was ~10-8 W/√Hz. Use of a fast, cooled detector such as an HEB or a Ga:GE photodetector, with NEP 10-12 W/√Hz would result in dramatic improvements in linewidth.

2.3 Wavelength Modulation Spectroscopy Using DFB QCLs

Utilizing DFB QCLS for traditional absorption spectroscopy has been an ongoing goal due to the lack of suitable source in the ≥ 3 THz spectral range. The high power and continuous tunability of QCLs make them an attractive source for elucidating the intermolecular behavior of chemically relevant species such as water and water-hydrocarbon clusters through probing their energy level structures. To that end a new QCL based spectrometer for pulsed gas expansions of methanol has recently been reported [21]**.** In brief, a single QCL device's voltage is scanned across its entire operating range. The beam is passed through a sample chamber in which a supersonic pulse of seed gas in argon is present. Gated integrators record the signal present form the pulsed gas and provide background subtraction. Characterization of a methanol system showed that the resolution and sensitivity of the QCL are on the ppm level, which was comparable to previous FIR gas lasers employed while simultaneously greatly simplifying the experimental setup.

Further development of the spectrometer has lead to several relevant improvements since that report. The primary improvement has been the result of the incorporation of a mulitpass cell within the sample chamber leading to a full order of magnitude enhancement in the setup's sensitivity to ca. $4 \cdot 10^{-7}$, which approached the shot noise limit of the detector of $3.51 \cdot 10^{-8}$. This enhanced sensitivity will allow for the detection of important water cluster systems, which have been difficult or impossible to measure due to their sub-trace concentration in the gas pulse (i.e. water hexamer, octamer, etc.). With this new setup water clusters are currently being studied in the 3.8 THz region.

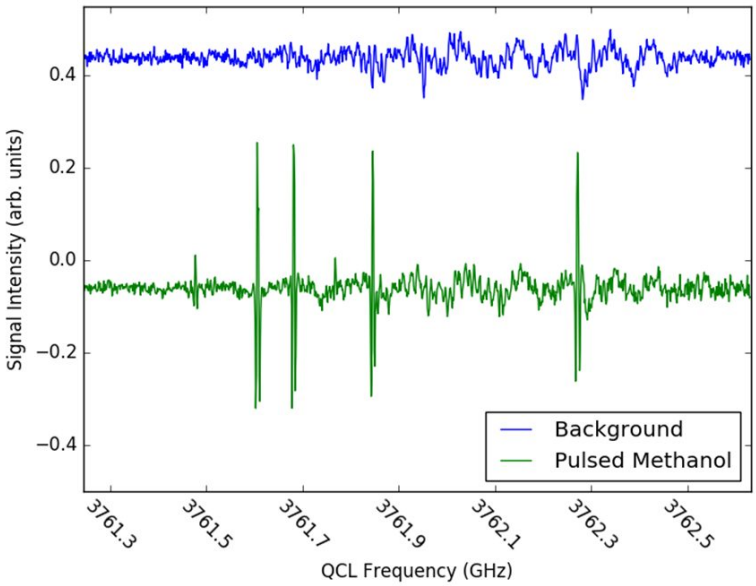

Figure 7: Spectrum obtained from vacuum chamber with no methanol (blue) and methanol being pulsed through a supersonic expansion (green) with an arbitrary offset. The periodic features in the background spectra are etalons that could not be removed from the spectra by background subtraction. The methanol spectrum shows the characteristic second derivation peak shape for the

absorption features. The sub-Doppler broadened linewidths (~5 Mhz) are consistent with previous experiments displaying rotational cooling to 4K. Methanol was chosen as a test gas for comparison to our previously reported work.

2.4 Tunable Frequency QCLs

The small width of the laser ridge (~ 10 µm) relative to the wavelength (~ 100 µm) has enabled DFB THz QCLs to be frequency tuned in novel ways [9]: by mechanically interacting with the optical mode extending from the width of the waveguide, the frequency of the QCL can be perturbed (see Figure 8 part a). The perturbation must be physically actuated, and a gold coated silicon MEMS plunger (part b) is mechanically pushed through an actuator shaft (part c) towards the DFB QCL, which has lead to frequency tuning of 300 GHz or 7.5% of the central 4 THz frequency[22].

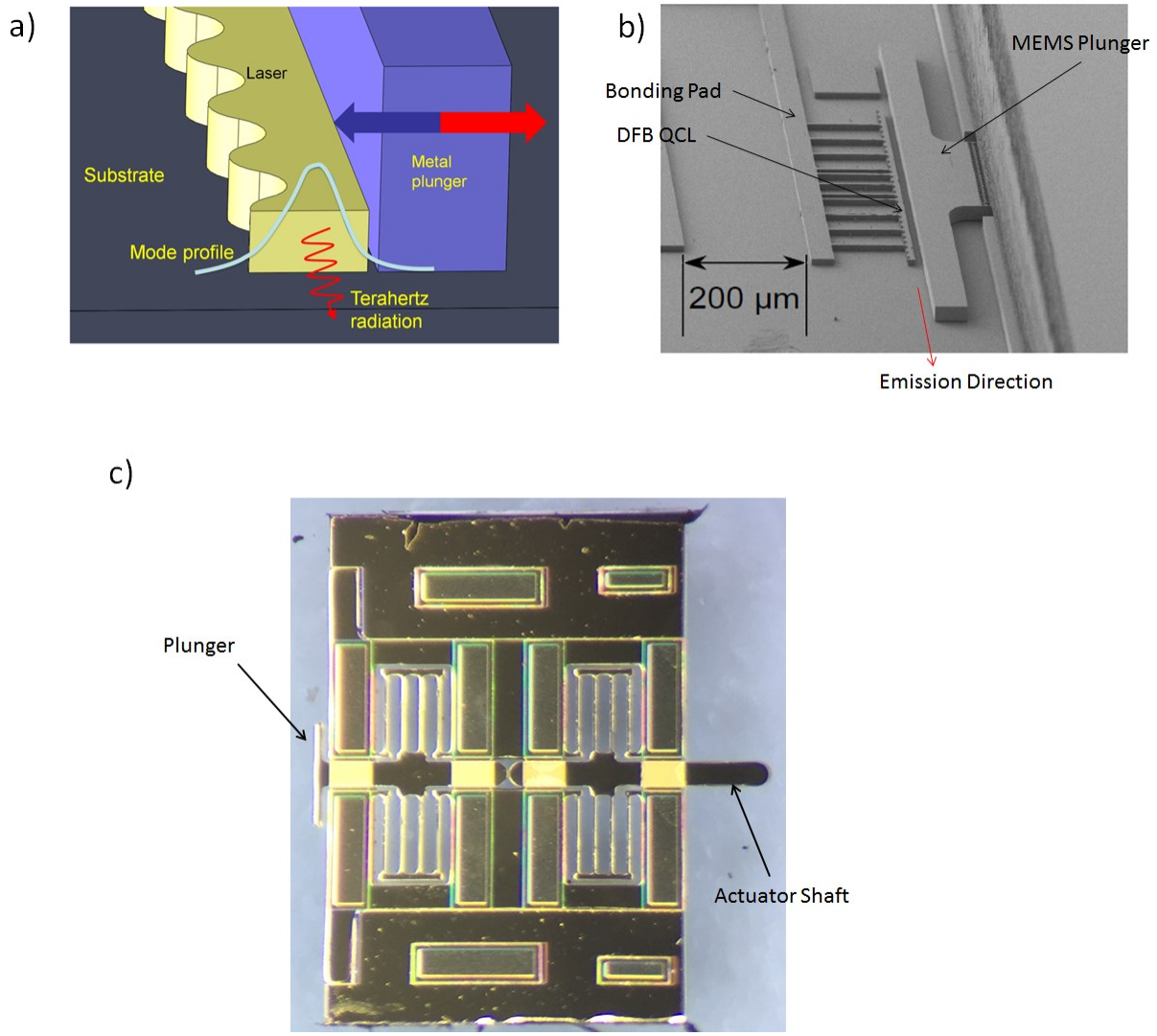

Figure 8 Part (a) shows a THz DFB QCL in close proximity to a moveable metal plunger. When the plunger is close the QCL, the optical mode is forced into the QCL causing blue shift tuning. Part (b) shows an SEM of the DFB QCL with the MEMS plunger bonded on top. Part (c) shows the MEMS plunger prior to bonding. The Actuator shaft is held in place by a MEMS spring structure, and pushing the actuator shaft causes the plunger to move toward the QCL.

In previous efforts this MEMS actuator shaft (and hence the tuning) was affected by either an external mechanical micrometer [22] or with a cryogenic motor with unknown absolute position [23]. Here we have implemented absolute position measurement of the MEMS plunger using a position sensitive device (PSD, First Sensor, OD6-6) operated at 47 K. The fixture to actuate the tunable THz DFB QCL is shown in Figure 9 , the fixture consists of a cryogenic temperature operable piezo motor stage (Micronix PP-17) with an attached copper arm to transfer the movement of the stage to the MEMS plunger; an adjustable spring-loaded pogo pin (home switch) with a corresponding contact pad for coarse contact proximity detection; and the PSD with laser diode (650nm) for fine positioning. The necessity for such a complex setup comes from the fact that stepping size of piezo stage is a strong function of temperature and the friction forces. For example, the stepping size is reduced by a factor of 3 when the operating temperate of the stage is reduced from room temperature (300K) to cryogenic temperature (47 K). The inclusion of the PSD and the proximity detecting home switch allows for absolute positioning with <1 μm error.

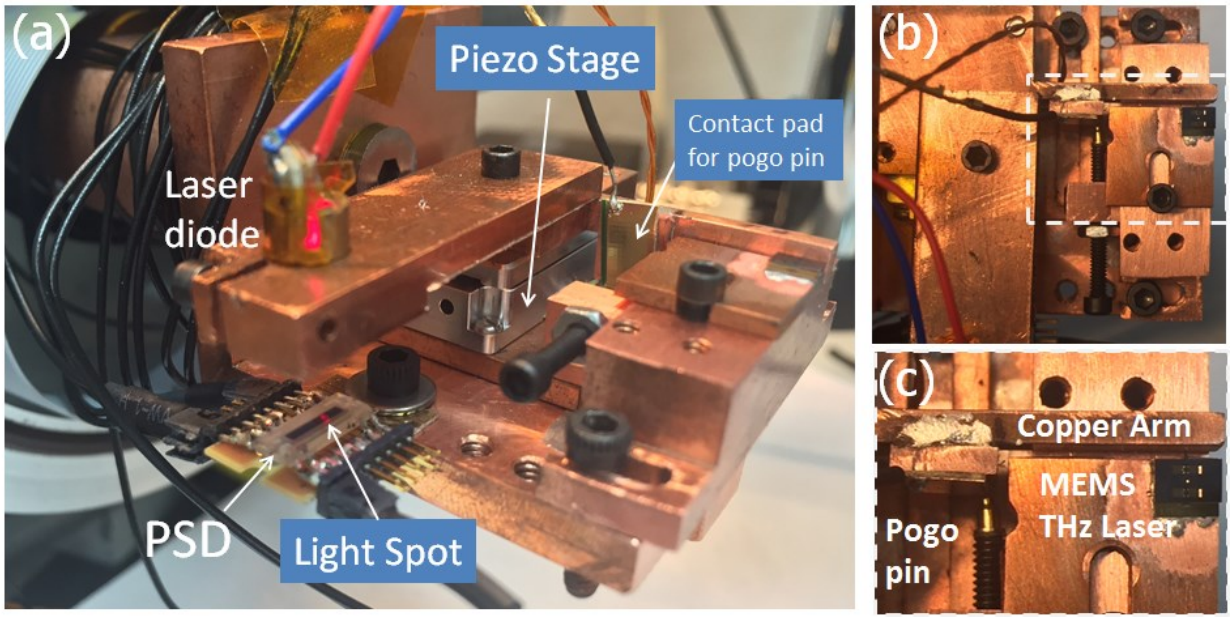

Figure 9: Overview of a tunable THz QCL device showing the piezo motor stage. The piezo motor is attached to the copper arm, which touches the MEMS plunger. Proximity to the MEMS plunger is determined cryogenically through a contact pogo switch. Fine positioning is determined by a position sensitive device (PSD) which is illuminated by a 650 nm laser.

ACKNOWLEDGEMENTS

This work was supported under National Science Foundation SBIR IIP/1330955 and NASA SBIR NNX15CP15C.

REFERENCES

[1] C. o. E. Science, A. f. S. A. C. Assessment, S. f. t. Future *et al.*, [Earth Science and Applications from Space: National Imperatives for the Next Decade and Beyond] The National Academies Press, (2007).

[2] J. W. Waters, L. Froidevaux, R. S. Harwood *et al.*, "The Earth observing system microwave limb sounder (EOS MLS) on the aura Satellite," Geoscience and Remote Sensing, IEEE Transactions on, 44(5), 1075-1092 (2006).
[3] S. Heyminck, U. U. Graf, R. Güsten *et al.*, "GREAT: the SOFIA high-frequency heterodyne instrument," A&A, 542, L1 (2012).
[4] [Stratospheric Terahertz Observatory], (2012).
[5] H. W. Hubers, "Terahertz Heterodyne Receivers," Selected Topics in Quantum Electronics, IEEE Journal of, 14(2), 378-391 (2008).
[6] E. Mueller, R. Henschke, J. Robotham, WE *et al.*, "Terahertz local oscillator for the Microwave Limb Sounder on the Aura satellite," Applied Optics, 46(22), 4907-4915 (2007).
[7] H. W. Hübers, A. Semenov, H. Richter *et al.*, "Heterodyne receiver for 3-5 THz with hot-electron bolometer mixer." 5498, 579-586.
[8] L. Li, L. Chen, J. Zhu *et al.*, "Terahertz quantum cascade lasers with> 1 W output powers," Electronics Letters, 50(4), 309-311 (2014).
[9] Q. Qin, B. S. Williams, S. Kumar *et al.*, "Tuning a terahertz wire laser," Nat Photon, 3(12), 732-737 (2009).
[10] A. W. M. Lee, B. S. Williams, S. Kumar *et al.*, "Tunable Terahertz Quantum Cascade Lasers with External Gratings," Optics Letters, 35(7), 910 - 912 (2010).
[11] H.-W. Hübers, S. Pavlov, H. Richter *et al.*, "High-resolution gas phase spectroscopy with a distributed feedback terahertz quantum cascade laser," Applied Physics Letters, 89(6), 061115 (2006).
[12] S. Kumar, Q. Hu, and J. L. Reno, "186 K operation of terahertz quantum-cascade lasers based on a diagonal design," Applied Physics Letters, 94(13), 131105 (2009).
[13] T.-Y. Kao, Q. Hu, and J. L. Reno, "Perfectly phase-matched third-order distributed feedback terahertz quantum-cascade lasers," Optics Letters, 37(11), 2070-2072 (2012).
[14] Q. Hu, A. W. M. Lee, and T. Y. Kao, [Efficient third-order distributed feedback laser with enhanced beam pattern], (2013).
[15] Q. Hu, B. S. Williams, S. Kumar *et al.*, "Resonant-phonon-assisted THz quantum-cascade lasers with metal-metal waveguides," Semiconductor Science and Technology, 20(7), 228 - 36 (2005).
[16] B. S. Williams, S. Kumar, Q. Hu *et al.*, "Distributed-feedback terahertz quantum-cascade lasers with laterally corrugated metal waveguides," Optics Letters, 30(21), 2909 - 11 (2005).
[17] M. I. Amanti, FischerM, ScalariG *et al.*, "Low-divergence single-mode terahertz quantum cascade laser," Nat Photon, 3(10), 586-590 (2009).
[18] T.-Y. Kao, X. Cai, A. W. M. Lee *et al.*, "Antenna coupled photonic wire lasers," Optics Express, 23(13), 17091-17100 (2015).
[19] P. Chen, E. A. Cohen, T. J. Crawford *et al.*, [JPL Millimeter and Submillimeter Spectral Line Catalog] NASA, Pasadena(2012).
[20] D. J. Hayton, A. Khudchenko, D. G. Pavelyev *et al.*, "Phase locking of a 3.4 THz third-order distributed feedback quantum cascade laser using a room-temperature superlattice harmonic mixer," Applied Physics Letters, 103(5), - (2013).
[21] W. T. S. Cole, N. C. Hlavacek, A. W. M. Lee *et al.*, "A Terahertz VRT spectrometer employing quantum cascade lasers," Chemical Physics Letters, 638, 144-148 (2015).
[22] Q. Qin, J. L. Reno, and Q. Hu, "MEMS-based tunable terahertz wire-laser over 330 GHz," Optics Letters, 36(5), 692-694 (2011).
[23] N. Han, A. de Geofroy, D. P. Burghoff *et al.*, "Broadband all-electronically tunable MEMS terahertz quantum cascade lasers," Optics Letters, 39(12), 3480-3483 (2014).